

Supplement of Atmos. Chem. Phys., 19, 3325–3339, 2019
<https://doi.org/10.5194/acp-19-3325-2019-supplement>
© Author(s) 2019. This work is distributed under
the Creative Commons Attribution 4.0 License.



Supplement of

The effect of hydrophobic glassy organic material on the cloud condensation nuclei activity of particles with different morphologies

Ankit Tandon et al.

Correspondence to: Markus D. Petters (markus_petters@ncsu.edu)

The copyright of individual parts of the supplement might differ from the CC BY 4.0 License.

Overview

Section S1 contains supporting data for the CCN experiments, including the relationship between instrument nominal temperature gradient and instrument supersaturation and experiments used to constrain the CCN activity of polyethylene particles. Section S2 contains tabulated data. Tables S1-S8 summarize data needed to reproduce Figures 2-5 in the main manuscript and Figures S1-S2 in this document.

Section S1. CCN Experiments

Figure S1 shows the relationship between instrument nominal temperature gradient and instrument supersaturation from the ammonium sulfate calibration. The experiment was performed using a TSI 3080 long DMA column, a TSI 3771 condensation particle counter and the DMT CCN instrument operated at a flow rate of 0.3 L min^{-1} . Note that the calibration was performed on a different DMA/CCN/CPC setup than the experiments performed in the main paper, which used the radial DMA and TSI 3020, which are used as detector for the coagulation instrument.

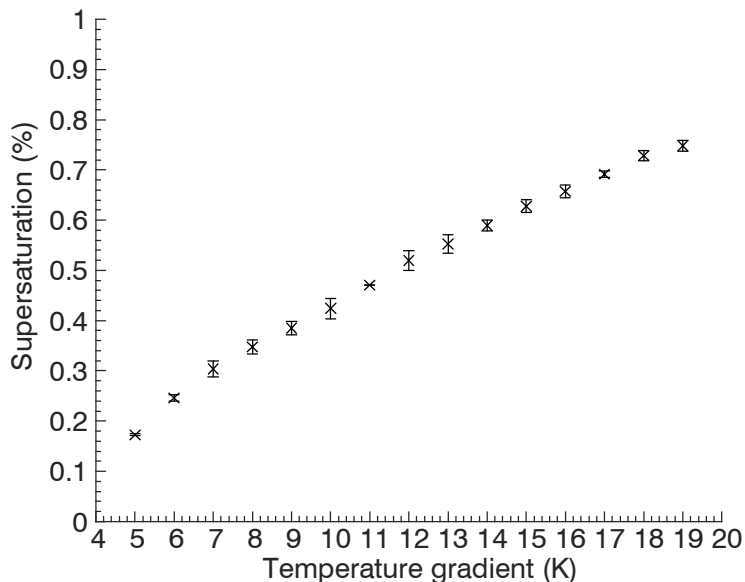


Figure S1. Relationship between instrument nominal temperature gradient and instrument supersaturation from the ammonium sulfate calibration at CCNc flow rate 0.3 L min^{-1} . Vertical bars show the standard deviation of the inferred supersaturation.

Figure S2 summarizes the experiments used to constrain the CCN activity of polyethylene particles. Here the CCNc was operated at the highest achievable supersaturation corresponding to $dT = 20 \text{ K}$ and a flow rate of 1 L min^{-1} . Experiments were performed using a high-flow DMA column to extend the diameter range to 750 nm . The concentration of 1 cm^{-3} CCN particles corresponds to the noise floor of the measurement in this experiment. For the glucose experiment, the fraction of particles activating at $D < 100 \text{ nm}$ is less than unity. This is due to losses in the inlet system. The activated fraction at 23.4 nm is 0.68 (Table S6); glucose particles of that size are still CCN active.

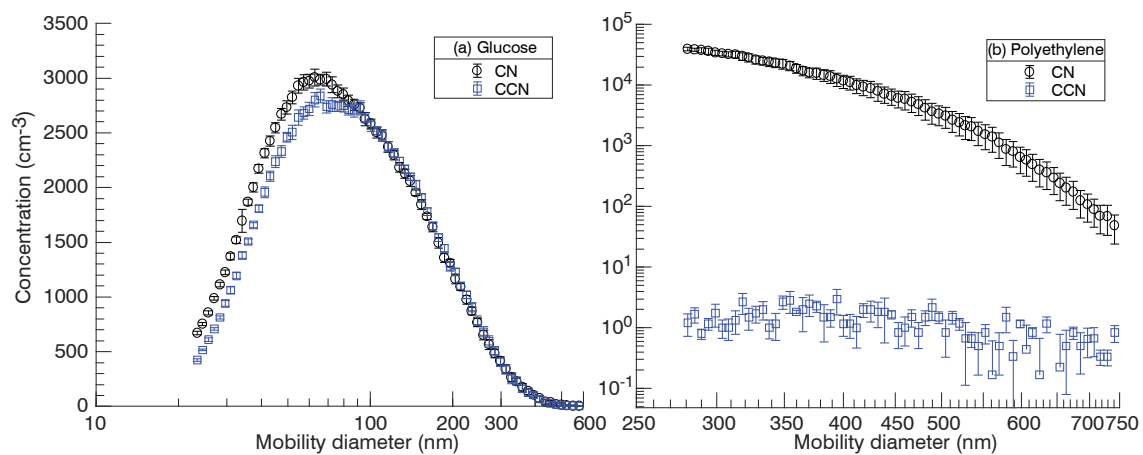


Figure S2. CCN experiments using (a) glucose and (b) polyethylene at $dT = 20\text{K}$ and CCNc flow rate 1.0 L min^{-1} .

Section S2. Data Tables

Table S1a. Data for Figure 2a, left panel in the main text. Columns are midpoint temperature of the 3K bin, mean particle geometry factor of all particles within the bin, standard deviation of particle geometry factor, and relative humidity in the RDMA. The fitted logistic curve and uncertainty in the inferred parameters is given in Table 1 of the main text.

T [°C]	ξ (-)	$\pm\xi$ (-)	RH (%)
25.5	5.02	0.37	3.23
28.5	4.13	0.32	3.21
31.5	4.02	0.22	3.18
34.5	4.71	0.75	3.13
37.5	3.98	0.05	3.07
40.5	3.96	0.16	3.02
43.5	3.86	0.28	3.02
46.5	3.80	0.15	3.07
49.5	3.52	0.11	3.06
52.5	3.46	0.32	2.82
55.5	3.21	0.13	2.91
58.5	3.10	0.10	3.01
61.5	2.89	0.13	3.02
64.5	2.90	0.22	2.99
67.5	2.78	0.64	2.95
70.5	2.29	0.25	2.85
73.5	2.24	0.12	2.81
76.5	1.83	0.06	2.82
79.5	1.20	0.34	2.86
82.5	1.08	0.11	2.85
85.5	0.72	0.39	2.79
88.5	1.02	0.01	2.74
91.5	1.11	0.20	2.69
94.5	0.86	0.59	2.68

Table S1b: Data for Figure 2b, left panel in the main text. Columns are midpoint temperature of the 3K bin, mean particle geometry factor of all particles within the bin, standard deviation of particle geometry factor, and relative humidity in the RDMA. The fitted logistic curve and uncertainty in the inferred parameters is given in Table 1 of the main text.

T [°C]	ξ (-)	$\pm\xi$ (-)	RH (%)
25.5	4.20	0.72	4.19
28.5	4.43	0.40	4.14
31.5	3.80	0.42	4.06
34.5	4.25	0.15	3.96
37.5	4.45	0.49	3.86
40.5	3.68	0.25	3.75
43.5	4.26	0.27	3.62
46.5	3.42	0.14	3.47
49.5	3.66	0.65	3.30
52.5	3.03	0.64	3.06
55.5	3.15	0.62	2.84
58.5	3.04	0.13	2.64
61.5	2.79	0.02	2.43
64.5	2.63	0.33	2.23
67.5	2.19	0.27	2.03
70.5	1.86	0.68	1.87
73.5	1.21	0.21	1.59
76.5	1.40	0.17	1.42
79.5	0.90	0.26	1.34
82.5	0.96	0.13	1.26
85.5	0.91	0.11	1.20
88.5	0.83	0.19	1.08
91.5	1.08	0.62	1.01
94.5	1.24	0.21	0.97

Table S2a: Data for Figure 3a in the main text. Activation properties of ammonium sulfate monomers of 50 nm mode diameter over three different temperature gradients of the CCNc column corresponding to three different water supersaturation levels (%).

Dp (nm)	dT = 8K		dT = 12K		dT = 16 K	
	CN (cm ⁻³)	CCN (cm ⁻³)	CN (cm ⁻³)	CCN (cm ⁻³)	CN (cm ⁻³)	CCN (cm ⁻³)
117.8	64.1	51.1	62.4	52.2	62.9	51.6
113.3	80.1	64.4	70.9	71.4	73.7	57.6
109.6	82.3	77.2	79.9	78.3	80.9	69.8
106.1	96.8	81.2	95.1	69.9	94.2	87.2
102.1	112.0	93.0	104.5	107.6	101.6	93.5
98.4	125.8	108.0	115.5	107.2	120.2	128.5
94.8	141.3	120.3	136.4	111.1	133.3	125.3
91.3	152.4	122.1	148.7	140.8	146.2	137.6
88.4	172.3	145.7	162.2	149.2	150.2	126.4
85.6	181.0	169.9	184.8	131.7	168.1	139.4
82.6	210.6	155.6	205.9	206.5	201.2	202.2
79.6	243.0	212.8	234.6	229.5	228.9	228.7
76.8	281.4	247.6	274.1	195.7	272.6	249.8
74.0	307.3	270.8	308.9	298.0	299.2	321.1
71.4	334.7	245.9	322.1	332.8	308.5	310.5
68.9	315.3	234.9	312.3	250.9	295.8	235.9
66.5	274.6	173.6	263.4	240.8	263.7	250.4
64.2	232.5	184.9	227.2	213.1	225.9	188.4
61.9	210.3	146.7	210.8	162.4	210.1	147.6
59.8	241.9	72.7	232.3	172.2	222.7	239.5
57.7	329.0	26.4	320.6	266.4	316.6	289.8
55.7	481.3	25.7	469.9	384.6	456.4	405.1
53.8	632.3	25.8	630.9	463.9	619.8	605.0
52.0	799.8	22.1	765.4	503.1	751.1	745.0
50.2	874.5	24.9	845.2	484.0	852.0	835.0
48.3	866.2	23.3	852.6	287.1	849.8	842.0
46.4	749.3	17.2	754.9	198.9	751.0	660.7
44.8	587.4	13.4	585.6	97.1	576.2	535.0
43.3	400.9	4.8	389.1	39.4	379.9	334.5
41.9	244.7	5.4	228.2	18.4	227.3	180.1
40.4	132.7	0.0	124.2	9.1	120.7	65.7
39.1	70.9	0.5	64.3	18.3	63.8	37.7
37.6	46.1	1.3	40.8	19.0	40.4	34.4
36.2	42.6	0.5	39.5	16.7	39.2	27.8
35.0	39.1	0.0	39.4	15.1	35.6	31.0
33.8	36.1	0.0	35.3	7.6	33.9	25.8
32.7	30.3	0.0	28.7	4.3	27.3	16.1
31.5	21.9	0.0	20.2	1.7	19.0	12.1
30.3	12.0	0.5	11.1	0.5	9.6	7.0

Table S2b: Data for Figure 3b in the main text. Activation properties of AS-PE coalesced particles at 25 °C, probably present in dimer morphology, over three different temperature gradients of the CCNc column corresponding to three different water supersaturation levels (%).

Dp (nm)	dT = 8K		dT = 12K		dT = 16 K	
	CN (cm ⁻³)	CCN (cm ⁻³)	CN (cm ⁻³)	CCN (cm ⁻³)	CN (cm ⁻³)	CCN (cm ⁻³)
117.8	0.3	0.6	0.2	1.1	0.4	0.0
113.3	0.5	0.0	0.4	1.1	0.3	1.6
109.6	0.4	0.7	0.7	0.0	0.4	0.0
106.1	0.6	0.5	0.7	0.5	0.7	0.5
102.1	0.9	0.5	1.2	1.6	0.9	2.1
98.4	0.7	2.1	1.3	1.1	1.7	0.0
94.8	1.7	0.5	1.8	1.6	1.3	0.5
91.3	1.9	1.1	1.3	0.5	1.7	1.6
88.4	1.4	0.7	1.5	2.9	1.1	0.7
85.6	1.5	0.5	1.5	0.5	1.7	1.1
82.6	2.3	0.5	2.1	1.1	1.7	0.7
79.6	4.2	0.0	2.8	3.8	2.5	0.8
76.8	8.2	0.0	5.9	4.8	5.8	12.3
74.0	12.2	0.0	10.6	8.6	9.8	9.7
71.4	19.1	1.1	17.1	8.1	15.6	15.1
68.9	26.3	0.0	21.8	16.4	19.5	21.9
66.5	30.5	0.0	23.9	15.0	26.4	24.0
64.2	26.9	0.0	24.5	14.4	24.9	25.4
61.9	25.3	0.0	21.4	8.5	23.4	24.2
59.8	19.7	1.1	16.6	6.9	18.8	14.5
57.7	14.0	0.0	14.2	1.6	12.3	5.9
55.7	9.6	0.0	8.0	1.1	8.9	4.8
53.8	6.1	0.0	4.9	1.1	5.8	4.8
52.0	5.0	0.0	3.8	1.1	3.8	0.8
50.2	3.5	0.0	3.4	1.6	3.2	0.8
48.3	3.8	0.0	3.2	0.9	2.6	2.6
46.4	3.2	0.0	2.7	2.2	3.0	1.6
44.8	2.8	0.0	2.5	0.0	2.3	2.2
43.3	2.3	0.0	2.2	0.0	2.5	4.8
41.9	1.8	0.0	1.7	0.5	1.0	1.1
40.4	0.7	0.0	0.9	0.0	1.5	1.1
39.1	1.0	0.0	0.4	0.0	0.6	0.5
37.6	0.3	0.0	0.2	0.0	0.5	0.0
36.2	0.3	0.0	0.1	0.5	0.1	0.0
35.0	0.2	0.0	0.1	0.0	0.1	0.0
33.8	0.1	0.0	0.0	0.5	0.1	0.0
32.7	0.0	0.0	0.1	0.0	0.1	0.0
31.5	0.0	0.0	0.0	0.0	0.0	0.0
30.3	0.0	0.0	0.0	0.5	0.0	0.0

Table S2c: Data for Figure 3c in the main text. Activation properties of AS-PE coagulated particles at 95 °C, most likely present in core-shell morphology, over three different temperature gradients of the CCNc column corresponding to three different water supersaturation levels (%).

Dp (nm)	dT = 8K		dT = 12K		dT = 16 K	
	CN (cm ⁻³)	CCN (cm ⁻³)	CN (cm ⁻³)	CCN (cm ⁻³)	CN (cm ⁻³)	CCN (cm ⁻³)
117.8	0.0	0.0	0.1	0.5	0.1	0.0
113.3	0.3	0.0	0.2	0.0	0.1	0.0
109.6	0.1	0.0	0.2	0.0	0.2	0.0
106.1	0.1	0.0	0.1	0.6	0.4	0.0
102.1	0.2	0.0	0.3	1.1	0.5	0.0
98.4	0.6	1.1	0.5	0.0	0.4	1.1
94.8	0.7	0.5	0.9	1.1	0.7	0.0
91.3	0.8	0.0	0.7	1.6	0.7	2.1
88.4	0.5	0.0	1.0	0.0	0.9	0.7
85.6	0.7	1.1	1.2	0.0	1.0	1.6
82.6	0.7	1.6	0.9	1.5	0.9	1.1
79.6	0.9	0.5	1.0	2.3	1.3	0.0
76.8	1.1	1.1	1.5	1.6	1.9	0.5
74.0	2.3	0.0	2.6	2.1	3.1	5.4
71.4	3.2	0.0	4.8	3.8	5.7	4.3
68.9	6.0	0.0	8.3	5.3	7.1	6.5
66.5	10.5	0.0	12.0	11.2	12.4	13.2
64.2	14.2	0.0	14.1	10.3	15.4	18.2
61.9	17.7	0.0	15.5	10.1	16.9	16.5
59.8	18.5	0.0	17.5	8.0	17.9	16.1
57.7	17.2	0.0	14.1	5.9	15.0	17.2
55.7	15.5	0.0	13.0	4.0	13.4	12.3
53.8	10.6	0.0	9.2	0.0	10.8	7.2
52.0	8.0	0.0	6.0	1.1	7.1	4.2
50.2	5.3	0.0	4.4	0.0	4.7	2.7
48.3	3.3	0.0	2.6	0.9	2.5	0.4
46.4	1.7	0.0	2.1	0.5	2.7	0.0
44.8	1.9	0.0	1.5	1.1	1.5	1.6
43.3	1.6	0.0	1.2	0.0	1.6	0.5
41.9	0.9	0.0	0.8	0.5	1.1	0.0
40.4	1.4	0.0	0.8	0.0	1.0	1.1
39.1	1.0	0.0	0.5	0.5	0.8	1.1
37.6	0.8	0.0	0.6	0.4	0.3	0.0
36.2	0.6	0.0	0.2	0.0	0.3	0.0
35.0	0.3	0.0	0.4	0.0	0.2	0.0
33.8	0.0	0.0	0.1	0.0	0.1	0.0
32.7	0.0	0.0	0.1	0.0	0.1	0.0
31.5	0.0	0.0	0.0	0.0	0.1	0.3
30.3	0.0	0.0	0.0	0.0	0.0	0.0

Table S3: Data for Figure 4 in the main text. Activated Fraction (mean \pm standard deviation) of AS Monomers (50 nm), AS (50 nm) + PE (50 nm) coalesced particles, conditioned at 25 °C, to be present in dimer morphology and AS (50 nm) + PE (50 nm) coagulated particles, conditioned at 95 °C, to be present in core-shell morphology over different water supersaturation (%) levels.

Water supersaturation (%)	AS Monomers (50 nm)	AS (50 nm) + PE (50 nm) coalesced particles at 25 °C in Dimer morphology	AS (50 nm) + PE (50 nm) coagulated particles at 95 °C in Core-Shell morphology
0.30	0.01 \pm 0.01	0.00 \pm 0.00	0.00 \pm 0.00
0.34	0.02 \pm 0.00	0.00 \pm 0.00	0.01 \pm 0.01
0.38	0.03 \pm 0.01	0.02 \pm 0.02	0.01 \pm 0.01
0.42	0.04 \pm 0.01	0.03 \pm 0.03	0.03 \pm 0.03
0.46	0.17 \pm 0.10	0.19 \pm 0.07	0.18 \pm 0.10
0.50	0.39 \pm 0.06	0.51 \pm 0.08	0.55 \pm 0.12
0.54	0.76 \pm 0.02	0.65 \pm 0.08	0.68 \pm 0.11
0.58	1.00 \pm 0.10	0.89 \pm 0.08	0.85 \pm 0.02
0.62	1.01 \pm 0.02	1.02 \pm 0.07	0.80 \pm 0.06
0.66	1.00 \pm 0.01	0.87 \pm 0.11	0.87 \pm 0.10

Table S4: Data for Figure 5 in the main text. Activated Fraction (mean \pm standard deviation) of AS Monomers along with AS-PE coagulated particles, formed by the coalescence of 50 nm mode diameter AS and 50 nm, 60 nm, 80 nm, 100 nm and 120 nm mode diameter PE particles, conditioned at 95 °C to be present in core-shell morphology.

Water supersaturation (%)	AS Monomers (50 nm)	AS (50 nm) + PE (50 nm)	AS (50 nm) + PE (60 nm)	AS (50 nm) + PE (80 nm)	AS (50 nm) + PE (100 nm)	AS (50 nm) + PE (120 nm)
0.30	0.01 \pm 0.01	0.00 \pm 0.00	-	-	-	-
0.34	0.02 \pm 0.00	0.01 \pm 0.01	0.01 \pm 0.00	-	-	-
0.38	0.03 \pm 0.01	0.01 \pm 0.01	0.00 \pm 0.00	-	-	-
0.42	0.04 \pm 0.01	0.03 \pm 0.03	0.01 \pm 0.00	-	-	-
0.46	0.17 \pm 0.10	0.18 \pm 0.10	0.21 \pm 0.03	0.16 \pm 0.00	0.16 \pm 0.05	0.17 \pm 0.02
0.50	0.39 \pm 0.06	0.55 \pm 0.12	0.40 \pm 0.09	0.44 \pm 0.06	0.51 \pm 0.02	0.41 \pm 0.04
0.54	0.76 \pm 0.02	0.68 \pm 0.11	0.65 \pm 0.14	0.63 \pm 0.01	0.64 \pm 0.04	0.63 \pm 0.04
0.58	1.00 \pm 0.10	0.85 \pm 0.02	0.88 \pm 0.02	0.83 \pm 0.15	0.75 \pm 0.04	0.68 \pm 0.09
0.62	1.01 \pm 0.02	0.80 \pm 0.06	0.98 \pm 0.00	0.83 \pm 0.02	0.78 \pm 0.04	0.80 \pm 0.02
0.66	1.00 \pm 0.01	0.87 \pm 0.10	-	-	-	-

Table S5: Data for Figure S1. Data-set used to construct dT(K) vs SS(%) calibration curve using AS particles in DMT CCNc with a total flow rate of 0.3 L min⁻¹.

dT (K)	Dd ₅₀ (nm)	SS (%)
5	90.4 ± 0.6	0.17 ± 0.00
6	71.7 ± 1.2	0.25 ± 0.01
7	62.6 ± 2.1	0.30 ± 0.02
8	57.4 ± 1.5	0.35 ± 0.01
9	53.8 ± 1.2	0.38 ± 0.01
10	50.6 ± 1.5	0.42 ± 0.02
11	47.3 ± 0.0	0.47 ± 0.00
12	44.4 ± 1.0	0.52 ± 0.02
13	42.7 ± 0.9	0.55 ± 0.02
14	40.9 ± 0.5	0.59 ± 0.01
15	39.3 ± 0.5	0.63 ± 0.01
16	38.2 ± 0.5	0.66 ± 0.01
17	36.9 ± 0.2	0.69 ± 0.01
18	35.8 ± 0.3	0.73 ± 0.01
19	35.1 ± 0.3	0.75 ± 0.01

Table S6: Data for Figure S2a. Concentrations of Glucose particles as CN and as CCN are mean of nine different scans along with associated standard deviations.

Dp (nm)	CN (cm ⁻³)	CCN (cm ⁻³)	Dp (nm)	CN (cm ⁻³)	CCN (cm ⁻³)
579.9	6.7 ± 5.1	5.8 ± 3.4	116.2	2355.3 ± 48.2	2373.9 ± 45.8
549.7	12.0 ± 7.1	10.2 ± 5.0	110.5	2441.4 ± 50.4	2439.4 ± 47.8
521.4	18.9 ± 9.3	18.4 ± 8.4	105.7	2490.3 ± 47.8	2479.3 ± 38.9
498.3	28.9 ± 12.5	24.9 ± 10.7	100.6	2554.7 ± 41.7	2550.2 ± 50.5
476.5	39.4 ± 15.8	37.6 ± 17.5	95.8	2623.1 ± 62.1	2568.9 ± 44.5
455.9	54.3 ± 17.5	50.6 ± 18.1	91.8	2680.8 ± 45.4	2609.6 ± 64.9
436.2	73.8 ± 23.8	68.3 ± 19.6	87.4	2726.9 ± 49.8	2667.5 ± 60.9
414.6	101.1 ± 27.8	95.2 ± 23.1	83.3	2769.2 ± 50.8	2675.9 ± 50.7
394.2	136.0 ± 26.6	132.1 ± 28.2	79.8	2816.7 ± 58.9	2721.1 ± 56.3
377.6	173.6 ± 28.8	164.4 ± 29.5	76.1	2858.7 ± 57.0	2718.2 ± 46.7
359.4	220.9 ± 32.7	217.0 ± 34.0	72.6	2873.9 ± 74.2	2741.5 ± 62.5
342.2	275.3 ± 32.1	275.2 ± 34.6	69.3	2909.1 ± 62.0	2741.2 ± 55.8
328.2	326.0 ± 39.8	328.7 ± 42.4	65.8	2930.9 ± 47.8	2740.8 ± 63.7
312.8	401.5 ± 39.8	398.8 ± 40.9	62.8	2925.0 ± 76.9	2698.1 ± 65.0
298.2	471.1 ± 40.6	473.2 ± 41.0	59.9	2918.2 ± 62.0	2684.4 ± 62.0
284.5	545.4 ± 40.4	558.6 ± 40.7	57.2	2885.8 ± 70.5	2632.6 ± 55.4
271.5	630.6 ± 45.7	649.9 ± 50.2	54.7	2835.1 ± 66.4	2573.4 ± 69.6
259.3	727.1 ± 44.9	740.9 ± 48.4	51.9	2773.3 ± 59.0	2478.8 ± 64.7
246.1	833.0 ± 37.0	846.2 ± 44.1	49.6	2700.3 ± 60.6	2386.9 ± 45.3
235.2	927.2 ± 35.2	939.5 ± 40.5	47.4	2604.0 ± 51.6	2294.8 ± 52.5
224.9	1034.0 ± 38.4	1049.9 ± 32.2	45.1	2495.8 ± 44.8	2164.8 ± 54.2
213.8	1138.1 ± 33.8	1153.4 ± 33.5	43.1	2396.7 ± 46.4	2044.0 ± 45.8
204.6	1227.0 ± 44.2	1267.2 ± 31.1	41.2	2268.9 ± 41.5	1929.4 ± 47.6
195.9	1338.9 ± 35.9	1367.1 ± 44.2	39.2	2130.4 ± 40.5	1765.8 ± 29.8
186.5	1437.8 ± 42.0	1477.4 ± 32.4	37.5	1983.9 ± 41.6	1642.6 ± 24.1
177.6	1546.1 ± 49.0	1588.7 ± 34.0	35.8	1837.6 ± 27.6	1488.1 ± 22.7
169.2	1660.8 ± 40.9	1693.6 ± 37.0	34.1	1644.7 ± 102.9	1338.7 ± 28.0
161.4	1754.4 ± 29.0	1793.3 ± 34.2	32.5	1505.3 ± 31.5	1189.2 ± 27.8
153.9	1862.5 ± 42.7	1906.4 ± 38.3	30.9	1361.6 ± 29.5	1040.9 ± 31.0
146.8	1955.3 ± 23.8	1988.3 ± 38.4	29.6	1218.1 ± 22.7	924.5 ± 26.5
140.2	2041.1 ± 48.9	2070.2 ± 33.7	28.3	1097.7 ± 20.8	817.4 ± 15.6
133.9	2119.4 ± 40.5	2164.3 ± 39.8	27.0	973.8 ± 18.3	704.6 ± 10.7
127.9	2191.4 ± 42.2	2235.3 ± 36.2	25.7	845.4 ± 19.2	598.9 ± 16.3
122.2	2279.2 ± 40.7	2286.8 ± 40.3	24.4	730.2 ± 15.5	517.9 ± 7.0
			23.4	642.0 ± 15.2	438.8 ± 11.0

Table S7: Data for Figure S2b. Concentrations of PE particles as CN and as CCN are mean of three different scans along with associated standard deviations.

Dp (nm)	CN (cm ⁻³)	CCN (cm ⁻³)	Dp (nm)	CN (cm ⁻³)	CCN (cm ⁻³)
741.3	21.6 ± 24.3	0.6 ± 0.3	453.3	4771.7 ± 1911.6	1.3 ± 0.4
729.2	29.9 ± 35.0	0.4 ± 0.1	446.4	5180.8 ± 1965.3	1.7 ± 0.3
717.4	32.0 ± 34.4	0.4 ± 0.1	439.4	5699.5 ± 2151.9	1.9 ± 1.3
707.2	44.7 ± 43.5	0.6 ± 0.3	432.8	6230.8 ± 2491.2	1.0 ± 0.8
697.1	54.3 ± 52.2	0.7 ± 0.3	425.8	6971.3 ± 2690.3	1.9 ± 0.7
685.9	63.6 ± 60.1	0.5 ± 0.3	418.7	7525.0 ± 2565.4	1.4 ± 0.5
674.8	83.5 ± 85.5	0.9 ± 0.2	412.4	8178.3 ± 2739.9	1.2 ± 0.5
664.0	98.3 ± 98.7	0.6 ± 0.4	406.3	9225.8 ± 2892.4	1.7 ± 0.5
654.6	123.9 ± 115.4	0.7 ± 0.6	400.3	9879.2 ± 2921.6	1.5 ± 0.4
645.5	160.3 ± 138.8	0.3 ± 0.4	394.4	10470.8 ± 3104.3	2.1 ± 1.4
635.1	199.8 ± 172.6	0.8 ± 0.3	388.6	11424.2 ± 3252.3	1.8 ± 0.5
625.0	222.5 ± 190.9	0.7 ± 0.5	382.9	12409.2 ± 3200.4	1.7 ± 0.9
615.0	272.2 ± 235.1	0.7 ± 0.2	376.6	13417.3 ± 3280.4	1.8 ± 0.5
606.4	329.4 ± 271.8	0.6 ± 0.7	370.4	13991.7 ± 2969.7	1.9 ± 1.0
598.0	370.7 ± 297.1	1.2 ± 0.2	365.0	15041.7 ± 2954.1	1.6 ± 1.1
588.6	483.7 ± 364.7	0.7 ± 0.3	359.7	16133.3 ± 3137.1	1.8 ± 0.1
579.3	569.1 ± 402.3	0.8 ± 0.7	354.5	17383.3 ± 3599.7	1.9 ± 1.1
570.2	689.3 ± 502.9	0.5 ± 0.3	348.8	18520.0 ± 4031.8	2.0 ± 0.7
561.2	814.5 ± 625.6	0.7 ± 0.4	343.1	19558.3 ± 3881.4	1.4 ± 0.5
552.4	934.9 ± 680.9	0.7 ± 0.3	338.2	20841.7 ± 4007.1	0.9 ± 0.3
543.8	1084.7 ± 737.2	0.8 ± 0.3	333.4	22150.0 ± 3814.2	1.3 ± 0.7
535.3	1325.1 ± 866.5	0.6 ± 0.2	328.0	23253.3 ± 3953.8	1.2 ± 0.5
528.0	1415.9 ± 888.0	0.7 ± 0.6	322.8	25083.3 ± 4424.5	1.2 ± 0.6
520.9	1583.3 ± 960.2	0.9 ± 0.3	318.2	26558.3 ± 4189.6	1.7 ± 1.0
512.8	1841.4 ± 1003.0	1.1 ± 0.3	313.2	28320.0 ± 4073.5	0.9 ± 0.6
504.9	2190.0 ± 1186.1	0.8 ± 0.5	308.2	29408.3 ± 3280.1	0.8 ± 0.4
497.2	2388.6 ± 1214.8	1.2 ± 0.3	303.9	30858.3 ± 2982.9	0.7 ± 0.3
489.5	2639.2 ± 1377.3	1.3 ± 0.8	299.2	32486.7 ± 3403.1	0.9 ± 0.7
482.0	3048.3 ± 1522.7	1.1 ± 0.4	294.5	34066.7 ± 4043.4	1.4 ± 0.3
474.6	3538.3 ± 1691.0	0.6 ± 0.4	289.9	35760.0 ± 3412.2	0.6 ± 0.2
467.4	3951.7 ± 1802.4	1.2 ± 0.5	285.4	37091.7 ± 2552.3	1.1 ± 0.5
460.3	4412.5 ± 1947.5	1.1 ± 0.5	281.0	38000.0 ± 2529.1	1.3 ± 0.5

Table S8: Mobility diameter (nm) of AS and PE monomers along with AS-PE coagulated particles at two different conditioner temperatures (°C) over which AS-PE coagulated particles are expected to be present in Dimer morphology and Core-shell morphology, respectively. Here ‘n’ gives number scans averaged.

Conditioner Temperature (°C)	Mobility diameter (nm)			Expected Morphology
	AS monomer	PE monomer	AS-PE Coagulated	
25	49.29 ± 0.38 (n = 3)	49.76 ± 0.25 (n = 3)	65.09 ± 0.39 (n = 29)	Dimer morphology
95	49.64 ± 0.26 (n = 3)	50.13 ± 0.74 (n = 3)	60.67 ± 0.54 (n = 30)	Core-shell morphology